Applied Physics Letters

Narrow linewidth characteristics of interband cascade lasers

Cite as: Appl. Phys. Lett. **116**, 201101 (2020); https://doi.org/10.1063/5.0006823
Submitted: 06 March 2020 . Accepted: 05 May 2020 . Published Online: 18 May 2020

Yu Deng, Bin-Bin Zhao, Xing-Guang Wang, and Cheng Wang

Applied Physics Letters ARTICLE scitation.org/journal/apl

Narrow linewidth characteristics of interband cascade lasers

Cite as: Appl. Phys. Lett. **116**, 201101 (2020); doi: 10.1063/5.0006823
Submitted: 6 March 2020 · Accepted: 5 May 2020 ·
Published Online: 18 May 2020

Yu Deng,[1,2,3] Bin-Bin Zhao,[1,2,3] Xing-Guang Wang,[1,2,3] and Cheng Wang[1,a)]

AFFILIATIONS

[1]School of Information Science and Technology, ShanghaiTech University, Shanghai 201210, China
[2]Shanghai Institute of Microsystem and Information Technology, Chinese Academy of Sciences, Shanghai 200050, China
[3]University of Chinese Academy of Sciences, Beijing 100049, China

[a)]**Author to whom correspondence should be addressed:** wangcheng1@shanghaitech.edu.cn

ABSTRACT

Narrow-linewidth mid-infrared laser sources are highly demanding for high-resolution gas spectroscopy applications. Interband cascade lasers (ICLs) are power-efficient laser sources emitting in the mid-infrared range. This work unveils the low phase noise characteristics of distributed feedback ICLs driven by a battery source. We show that the measured spectral linewidth of ICLs is as narrow as 284 kHz (at a 1 ms observation time), which is smaller than those of common quantum cascade lasers. On the other hand, raising the pump current reduces the intrinsic linewidth down to 12 kHz. The linewidth broadening factor is in the range of 2.0–3.0, leading to a Schawlow–Townes linewidth as narrow as 1.6 kHz. This work suggests the high potential of developing battery-driven, high-resolution gas spectroscopy instruments using ICLs.

Semiconductor lasers exhibit finite spectral linewidth due to the existence of spontaneous emission, phase-amplitude coupling effect, and technical noise sources. The spontaneous emission leads to the well-known Schawlow–Townes linewidth $\Delta\nu_{st}$.[1] The phase-amplitude coupling effect is usually described by the linewidth broadening factor α (LBF, or alpha factor), which broadens the intrinsic linewidth to $\Delta\nu_{in} = \Delta\nu_{st}\ (1+\alpha^2)$.[2] On the other hand, technical noise sources, including current source noise, temperature fluctuation, and mechanical vibration, further broaden the total spectral linewidth. For coherent fiber-optical communication systems, the spectral linewidth of near-infrared semiconductor lasers significantly affects the signal quality and hence limits the data transmission rate. The spectral linewidth of quantum well lasers is usually in the MHz range. In comparison, quantum dot lasers are featured with a narrower spectral linewidth of around 100 kHz.[3,4] For gas sensing and molecular spectroscopy systems, quantum cascade lasers (QCLs) and interband cascade lasers (ICLs) are two major laser sources emitting in the mid-infrared spectral range where a large variety of molecules show strong absorption lines due to both rotation and vibration transitions.[5,6] The spectral linewidth of the two mid-infrared lasers can limit the resolution, accuracy, and sensitivity of gas spectroscopy systems.[7,8] The linewidth characteristics of QCLs have been widely investigated through the measurement of the frequency noise spectral power density (FNPSD). Owing to the near-zero LBF,[9,10] QCLs usually show a narrow intrinsic linewidth of hundreds of Hz.[11,12] However, the total spectral linewidth is broadened to the MHz range[13–15] due to the common technical noise sources, as well as the specified internal electrical noise.[16,17] In addition, various techniques have been developed to reduce the linewidth of QCLs, including the gas absorption line stabilization,[18] the high-finesse optical cavity stabilization,[19] the strong optical feedback stabilization,[20] as well as the popular optical frequency comb stabilization.[21] In contrast, there are very few reports on the linewidth properties of ICLs.

The stimulated emission of ICLs relies on the interband transition (such as quantum well lasers) of carriers in type-II quantum wells, while the cascading scheme is employed to enhance the gain such as QCLs.[22] In comparison with QCLs, the power consumption of ICLs is one or two orders of magnitude lower than typical QCLs,[23] which enables the battery-driven gas sensing instruments and the mission in Mars Curiosity rover.[24] Our recent work showed that the below-threshold LBF of one Fabry–Pérot ICL was in the range of 1.0–1.5, and the above-threshold LBF was in the range of 2.0–3.0.[25] This LBF is smaller than those of typical quantum well lasers (3.0–5.0)[1] but larger than those of typical QCLs (0–2.0).[9,10] The only report on the linewidth of a distributed feedback (DFB) ICL is from Borri *et al.*, where the ICL emits at 4.6 μm, and its intrinsic linewidth reduced down to

about 10 kHz with increasing pump current.[26] The total spectral linewidth was reported to be about 3.0 MHz over a 1.0 s observation time (1.5 MHz over 1.0 ms), but its dependence on the pump current was not reported. On the other hand, the Schawlow–Townes linewidth of ICLs is still unknown. In addition, ICLs have the best performance in the spectral range of 3.0–4.0 μm, in contrast to those beyond 4.0 μm.[27–29] In this work, we systematically investigate the linewidth characteristics of DFB ICLs emitting around 3.4 μm, including the total spectral linewidth, the intrinsic linewidth, as well as the Schawlow–Townes linewidth, through the measurement of FNPSDs as a function of the pump current.

The ICL under study is a single-mode DFB laser with a cavity length of 900 μm and a ridge width of 5.0 μm (from Nanoplus). The front facet is anti-reflection (AR) coated, while the rear facet is high-reflection (HR) coated. The ICL is pumped by a low-noise battery source (LDX-3620B) with a root mean square noise of less than 70 nA (over 100 Hz bandwidth). The operation temperature is controlled by a thermo-electric cooler, with a stability of $\pm$0.001 °C (over 1 h). As shown in Fig. 1(a), the output of the ICL is collimated by an aspherical lens and then split to two paths by a beam splitter. One path goes to a high-resolution (0.08/cm) Fourier transform infrared spectrometer (FTIR, Bruker) for measuring the optical spectrum. The other path goes to a gas cell with a length of 5.0 cm, which is filled with pure methane with a pressure of 7.4 Torr. The gas cell acts as a frequency discriminator, which converts the frequency noise of the laser into intensity noise. The converted intensity signal is detected by a HgCdTe photodetector with a nominal bandwidth of 560 MHz (Vigo), followed by a preamplifier with a low cutoff frequency of 1 kHz. The DC voltage is recorded by a digital oscilloscope, and the AC noise spectrum is measured by a broadband electrical spectrum analyzer (ESA). It is noted that the FTIR, the gas cell, and the photodetector are slightly misaligned with the ICL to avoid any residual optical feedback, which otherwise can significantly alter the frequency noise and hence the laser linewidth.[30]

Figure 1(b) shows that the lasing threshold I_{th} of the ICL increases from 17 mA at 15 °C up to 25 mA at 35 °C. Meanwhile, the maximum output power decreases from 22.1 mW down to 13.6 mW. At 20 °C, the optical wavelength in Fig. 1(c) increases with the pump current from 3.386 μm at 30 mA up to about 3.390 μm at 70 mA, and the corresponding current tunability on the lasing frequency is −2.82 GHz/mA. One absorption line of the methane gas cell centered at 3.392 μm is used as the frequency discriminator. In Fig. 1(d), the transmission line of the frequency discriminator is very carefully calibrated through tuning the wavelength of the ICL via changing the pump current, while the operation temperature is maintained at 23.53 °C. The measured transmission line (dots) is in good agreement with the HITRAN database (dashed line).[31] Throughout the frequency noise measurement, the optical power reaching the gas cell is maintained at 1.3 mW, using an adjustable diaphragm (Thorlabs, ID12). The diaphragm is misaligned with the optical path as well, in order to avoid any light reflection from the diaphragm to the laser cavity. Through linearly fitting the slope of the transmission line (solid line), the conversion factor for the frequency noise to the intensity noise is extracted to be 39.8 mV/MHz. The ICL frequency at a different pump current is always operated at the center of the linear slope by tuning the operation temperature, and the temperature tunability on the lasing frequency is −8.61 GHz/°C.

Before measuring the frequency noise of the ICL, the intensity noise contribution is first measured through tuning the lasing frequency out of the transmission line. Figure 2 shows that the intensity noise contribution is more than three orders of magnitude smaller than the frequency noise of the ICL, which means the sensitivity of the frequency discriminator is high enough and the intensity noise does not limit the frequency noise measurement. Figure 2 unveils that the FNPSD decreases up to about 1.0 MHz, following the typical 1/f trend. Above 1.0 MHz, the FNPSD is almost constant and reaches the intrinsic white noise level, which is around 10k Hz^2/Hz. It is worthwhile to mention that this trend is different from the FNPSD of typical QCLs, where the white noise is usually reached at frequencies above 10 MHz.[11,20,32] Raising the pump current in Fig. 2 reduces the white noise level as QCLs and common laser diodes. However, the 1/f noise increases with the pump current, which is out of expectation.

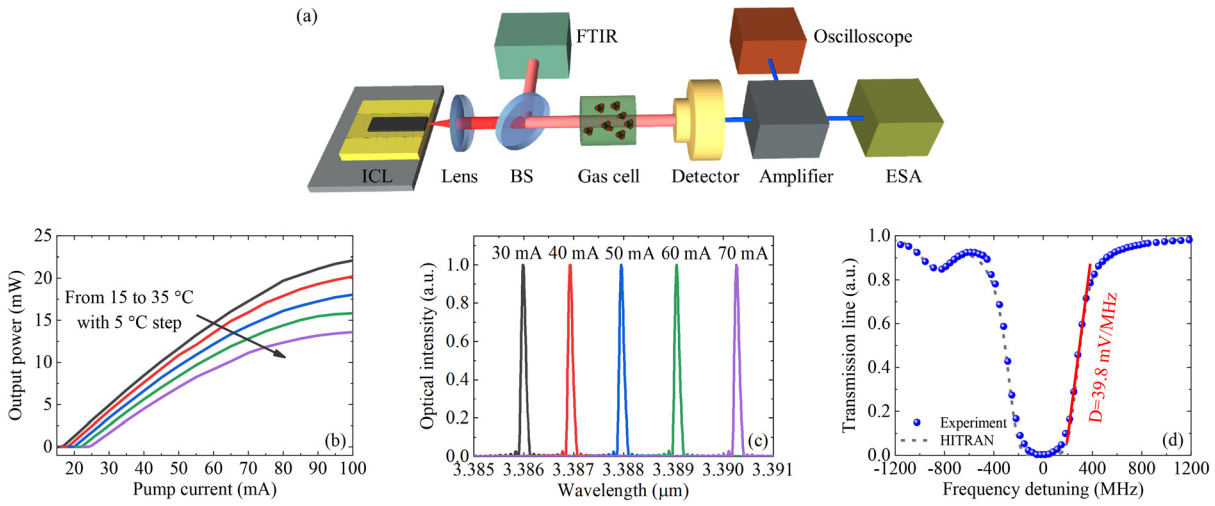

FIG. 1. (a) Experimental setup for frequency noise measurement. BS is beam splitter, FTIR is Fourier transform infrared spectrometer, and ESA is electrical spectrum analyzer. (b) L–I curves of the ICL at several operation temperatures. (c) Optical spectra for several pump currents at 20 °C. (d) Transmission line of the methane gas cell at 3.392 μm.

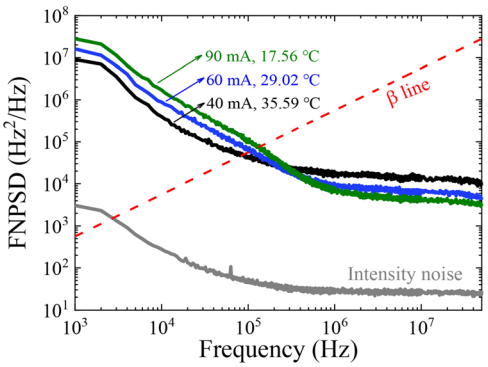

FIG. 2. FNPSD and intensity noise contribution of the ICL for several pump currents associated with the corresponding operation temperature.

Based on the β-separation line theory described in Ref. 33, the spectral linewidth of lasers can be determined by partial FNPSD with the amplitude above the β line (dashed line), as shown in Fig. 2. It is noted that the operation temperature is reduced when increasing the pump current, in order to maintain the lasing wavelength at the slope center of the transmission line in Fig. 1(d). Figure 3(a) shows that the spectral linewidth of the ICL (named as *ICL A*) first decreases from 478 kHz at 35 mA down to a minimum of 284 kHz at 45 mA (linewidth observation time is 1.0 ms). It is noted that the minimum spectral linewidth is achieved at about $1.8\times I_{th}$. Then, the spectral linewidth re-broadens significantly with an increasing pump current of up to more than 1.0 MHz, which is more than 3.5 times larger than the minimum value. Such a strong linewidth broadening behavior can be directly attributed to the rising $1/f$ noise observed in Fig. 2. In order to confirm the linewidth broadening characteristics, we measured another DFB ICL named as *ICL B* (see the supplementary material for details) in Fig. 3(b). Similar to the trend of *ICL A*, the spectral linewidth of *ICL B* first decreases from 517 kHz at 30 mA down to a minimum of 372 kHz at 35 mA and then re-broadens for higher pump currents. The linewidth re-broadening phenomenon is commonly

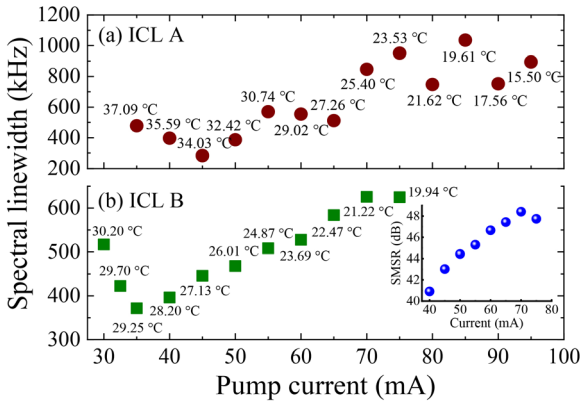

FIG. 3. Total spectral linewidth of (a) ICL sample A and (b) ICL sample B. The linewidth observation time is 1.0 ms, and the corresponding operation temperatures are listed in the figure. The inset shows the evolution of the side mode suppression ratio.

observed in high-power laser diodes. One main reason is the nonuniform carrier distribution due to both the longitudinal spatial hole burning effect and the lateral spatial hole burning effect.[34–36] The longitudinal hole burning effect is indeed strong for lasers with asymmetric AR/HR facet coatings, and this effect can be suppressed by using symmetric AR/AR facet coatings.[3,36,37] On the other hand, the lateral hole burning effect can be reduced by employing wider mesa.[38] The other common reason inducing the linewidth re-broadening is the mode partitioning between the main lasing mode and the side modes.[39,40] However, this is not the case for the measured ICL in this work, because the side mode suppression ratio (SMSR) increases with the pump current from 41 dB at 40 mA up to 48 dB at 70 mA [the inset of Fig. 3(b)]. It is remarked that the spectral linewidth of ICLs at a fixed pump current may decrease for a lower operation temperature.[3,4,41,42] Therefore, in case the ICLs are operated at a constant temperature for all the pump currents, the linewidth re-broadening effect can be more severe than that in Fig. 3. In addition, the measured linewidths of *ICL A* are more scattering than those of *ICL B*, which is likely due to the poorer frequency stability of *ICL A*. The frequency stability becomes even worse for pump currents higher than 75 mA due to Joule heating. Figure 4 compares the spectral linewidth of ICLs with those of free-running QCLs operated at room temperature.[13–15,17,18,21,26,32,43–45] It is found that the measured ICL linewidth of 284 kHz is generally narrower than typical QCL linewidths. This is mainly benefited from the lower $1/f$ noise in ICLs, thanks to the low-noise battery-driven source with lower pump current. Besides, the peculiar internal electrical noise in QCLs broadens the spectral linewidth as well, which might not occur in ICLs.[16,17] The narrow-linewidth feature of ICLs is of prime importance for high-resolution gas spectroscopy applications in the mid-infrared spectral range. Especially, ICLs exhibit superior performances in the 3.0–4.0 μm range, which is very challenging for QCLs to reach.

From the white-noise level N_w of the FNPSD in Fig. 2, the intrinsic linewidth can be easily obtained through the simple relation $\Delta\nu_{in} = \pi N_w$.[1] Using the N_w value averaged in the frequency range of 10–50 MHz, the extracted intrinsic linewidth $\Delta\nu_{in}$ of the ICLs is plot in Fig. 5. It shows that the intrinsic linewidth of *ICL A* decreases from 80 kHz at 35 mA down to about 12 kHz at 95 mA. In addition, the intrinsic linewidth of *ICL B* quantitatively matches well with *ICL A*. In comparison, QCLs usually exhibit an intrinsic linewidth of several hundred hertz, which is one or two orders of magnitude narrower

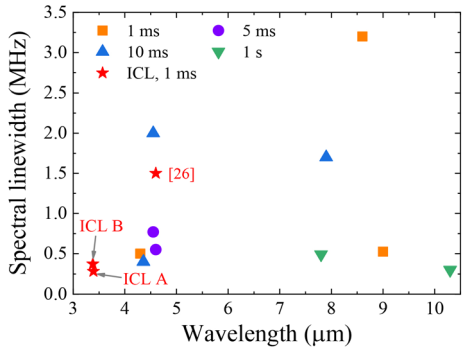

FIG. 4. Spectral linewidth comparison with QCLs operated at room temperature for different observation times.

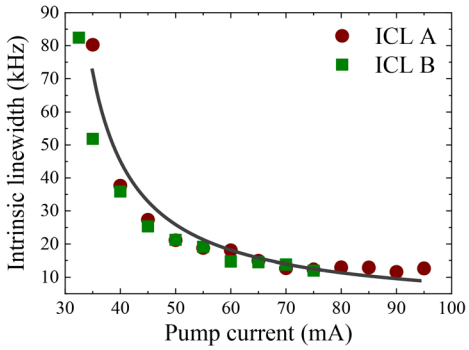

FIG. 5. Intrinsic linewidths of ICL samples. Solid line is the linewidth calculation using Eq. (1).

than the measured ICL ones.[11,32] The analytical relation between the intrinsic linewidth and the output power P_0 of semiconductor lasers is given by[1,46]

$$\Delta\nu_{in} = n_{sp}v_g^2\frac{\alpha_m\alpha_T h\nu}{4\pi P_0}(1+\alpha^2), \tag{1}$$

where n_{sp} is the population inversion factor, v_g is the group velocity, α_m is the mirror loss, α_T is the total cavity loss, and $h\nu$ is the photon energy. Using the set of parameters: $n_{sp}=1.05$, $\alpha_m=6.7$/cm, α_T=10/cm, $\alpha=2.6$, Eq. (1) well reproduces the intrinsic linewidth declining trend as a function of the pump current.

It is known that the intrinsic linewidth of semiconductor lasers is broadened by the LBF from the Schawlow–Townes linewidth by a factor of $(1+\alpha^2)$. In order to unveil the Schawlow–Townes linewidth of ICLs, we measured the above-threshold LBF using the self-mixing interferometry method.[25,47,48] This method uses a weak optical feedback with modulated phase to perturb the optical power of ICLs. The LBF is extracted based on the analysis of the self-mixing interferometric fringes of the output power, and the measurement details can be referred in Ref. 25. Figure 6(a) shows that the LBFs of both DFB ICL samples are in the range of 2.0–3.0, which is consistent with our previous measurement on a Fabry–Pérot ICL in Ref. 25. The LBF is almost independent of the pump current due to the gain clamping effect. Using the intrinsic linewidths in Fig. 5 and the LBFs in Fig. 6(a), the Schawlow–Townes linewidths of both ICLs are extracted in Fig. 6(b). It is shown that the Schawlow–Townes linewidth of *ICL A* declines from 14 kHz at 35 mA down to about 1.6 kHz at 95 mA, and that of *ICL B* is very similar to well. Such a small linewidth level is comparable to those of QCLs, considering their near-zero LBFs.[11]

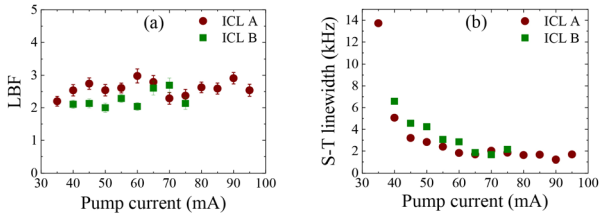

FIG. 6. (a) Linewidth broadening factors and (b) Schawlow–Townes linewidths of the ICL samples.

In summary, this work unveiled the phase noise characteristics of DFB ICLs driven by a battery source. It is found that the total spectral linewidth of ICLs is as narrow as 284 kHz, which is even smaller than common free-running QCLs. This is benefited from the lower $1/f$ noise in comparison with those of QCLs. The spectral linewidth exhibits a strong re-broadening behavior as a function of pump current, which is likely due to the spatial hole burning effect. The intrinsic linewidth of ICLs declines with an increasing pump current down to about 12 kHz, which is about one or two orders of magnitude higher than those of QCLs. In contrast to the usual near-zero LBF in QCLs, the LBF of ICLs is in the range of 2.0–3.0, which is almost independent of the pump current. The Schawlow–Townes linewidth of ICLs goes down to about 1.6 kHz with increasing pump current, which is comparable to those of QCLs. The narrow linewidth feature of battery-driven ICLs suggests its high superiority for power-efficient and high-resolution gas spectroscopy applications, especially in the spectral range of 3.0–4.0 μm. Future work will employ frequency stabilization techniques to narrow the spectral linewidth of ICLs down to the kHz level.

See the supplementary material for the device parameters and the static properties of ICL sample B.

This work was supported by the National Science Foundation of China (NSFC) (No. 61804095). The authors thank Nanoplus for providing basic device parameters of the ICL samples.

DATA AVAILABILITY

The data that supports the findings of this study are available within the article and its supplementary material.

REFERENCES

[1] L. A. Coldren, S. W. Corzine, and M. L. Mashanovitch, *Diode Lasers and Photonic Integrated Circuits* (John Wiley & Sons, 2012).
[2] C. H. Henry, IEEE J. Quantum Electron. **18**, 259 (1982).
[3] J. Duan, H. Huang, Z. G. Lu, P. J. Poole, C. Wang, and F. Grillot, Appl. Phys. Lett. **112**, 121102 (2018).
[4] T. Septon, A. Becker, S. Gosh, G. Shtendel, V. Sichkovskyi, F. Schnabel, A. Sengül, M. Bjelica, B. Witzigmann, J. P. Reithmaier *et al.*, Optica **6**, 1071 (2019).
[5] A. Kosterev, G. Wysocki, Y. Bakhirkin, S. So, R. Lewicki, M. Fraser, F. Tittel, and R. F. Curl, Appl. Phys. B **90**, 165 (2008).
[6] L. Dong, C. Li, N. P. Sanchez, A. K. Gluszek, R. J. Griffin, and F. K. Tittel, Appl. Phys. Lett. **108**, 011106 (2016).
[7] G. Wysocki, R. F. Curl, F. K. Tittel, R. Maulini, J. M. Bulliard, and J. Faist, Appl. Phys. B **81**, 769 (2005).
[8] I. Galli, M. Siciliani de Cumis, F. Cappelli, S. Bartalini, D. Mazzotti, S. Borri, A. Montori, N. Akikusa, M. Yamanishi, G. Giusfredi *et al.*, Appl. Phys. Lett. **102**, 121117 (2013).
[9] J. Faist, F. Capasso, C. Sirtori, D. L. Sivco, A. L. Hutchinson, and A. Y. Cho, Appl. Phys. Lett. **67**, 3057 (1995).
[10] J. Kim, M. Lerttamrab, S. L. Chuang, C. Gmachl, D. L. Sivco, F. Capasso, and A. Y. Cho, IEEE J. Quantum Electron. **40**, 1663 (2004).
[11] S. Bartalini, S. Borri, P. Cancio, A. Castrillo, I. Galli, G. Giusfredi, D. Mazzotti, L. Gianfrani, and P. D. Natale, Phys. Rev. Lett. **104**, 083904 (2010).
[12] M. S. Vitiello, L. Consolino, S. Bartalini, A. Taschin, A. Tredicucci, M. Inguscio, and P. De Natale, Nat. Photonics **6**, 525 (2012).
[13] L. Tombez, S. Schilt, D. Hofstetter, and T. Südmeyer, Opt. Lett. **38**, 5079 (2013).
[14] E. Fasci, N. Coluccelli, M. Cassinerio, A. Gambetta, L. Hilico, L. Gianfrani, P. Laporta, A. Castrillo, and G. Galzerano, Opt. Lett. **39**, 4946 (2014).

[15]I. Sergachev, R. Maulini, A. Bismuto, S. Blaser, T. Gresch, Y. Bidaux, A. Muller, S. Schilt, and T. Südmeyer, Opt. Lett. **39**, 6411 (2014).
[16]S. Borri, S. Bartalini, P. C. Pastor, I. Galli, G. Giusfredi, D. Mazzotti, M. Yamanishi, and P. De Natale, IEEE J. Quantum Electron. **47**, 984 (2011).
[17]L. Tombez, S. Schilt, J. Di Francesco, P. Thomann, and D. Hofstetter, Opt. Express **20**, 6851 (2012).
[18]F. Cappelli, I. Galli, S. Borri, G. Giusfredi, P. Cancio, D. Mazzotti, A. Montori, N. Akikusa, M. Yamanishi, S. Bartalini *et al.*, Opt. Lett. **37**, 4811 (2012).
[19]M. S. Taubman, T. L. Myers, B. D. Cannon, R. M. Williams, F. Capasso, C. Gmachl, D. L. Sivco, and A. Y. Cho, Opt. Lett. **27**, 2164 (2002).
[20]B.-B. Zhao, X.-G. Wang, and C. Wang, "Strong optical feedback stabilized quantum cascade laser," ACS Photonics (2020) (in press).
[21]B. Argence, B. Chanteau, O. Lopez, D. Nicolodi, M. Abgrall, C. Chardonnet, C. Daussy, B. Darquié, Y. Le Coq, and A. Amy-Klein, Nat. Photonics **9**, 456 (2015).
[22]R. Q. Yang, Superlattices Microstruct. **17**, 77 (1995).
[23]I. Vurgaftman, W. W. Bewley, C. L. Canedy, C. S. Kim, M. Kim, C. D. Merritt, J. Abell, J. R. Lindle, and J. R. Meyer, Nat. Commun. **2**, 585 (2011).
[24]C. R. Webster, P. R. Mahaffy, S. K. Atreya, J. E. Moores, G. J. Flesch, C. Malespin, C. P. McKay, G. Martinez, C. L. Smith, J. Martin-Torres *et al.*, Science **360**, 1093 (2018).
[25]Y. Deng, B.-B. Zhao, and C. Wang, Appl. Phys. Lett. **115**, 181101 (2019).
[26]S. Borri, M. S. de Cumis, S. Viciani, F. D'Amato, and P. De Natale, APL Photonics **5**, 036101 (2020).
[27]A. Spott, E. J. Stanton, A. Torres, M. L. Davenport, C. L. Canedy, I. Vurgaftman, M. Kim, C. S. Kim, C. D. Merritt, W. W. Bewley *et al.*, Optica **5**, 996 (2018).
[28]B. Schwarz, J. Hillbrand, M. Beiser, A. M. Andrews, G. Strasser, H. Detz, A. Schade, R. Weih, and S. Höfling, Optica **6**, 890 (2019).
[29]R. Q. Yang, L. Li, W. Huang, S. M. Shazzad Rassel, J. A. Gupta, A. Bezinger, X. Wu, S. G. Razavipour, and G. C. Aers, IEEE J. Sel. Top. Quantum Electron. **25**, 1200108 (2019).
[30]J. Ohtsubo, *Semiconductor Lasers: Stability, Instability and Chaos* (Springer, 2017).
[31]L. S. Rothman, I. E. Gordon, A. Barbe, D. C. Benner, P. E. Bernath, M. Birk, V. Boudon, L. R. Brown, A. Campargue, J. P. Champion *et al.*, J. Quant. Spectrosc. Radiat. Transfer **110**, 533 (2009).
[32]L. Tombez, J. Di Francesco, S. Schilt, G. Di Domenico, J. Faist, P. Thomann, and D. Hofstetter, Opt. Lett. **36**, 3109 (2011).
[33]G. Di Domenico, S. Schilt, and P. Thomann, Appl. Opt. **49**, 4801 (2010).
[34]M.-C. Wu, Y. Lo, and S. Wang, Appl. Phys. Lett. **52**, 1119 (1988).
[35]H. Wenzel, H. J. Wunsche, and U. Bandelow, Electron. Lett. **27**, 2301 (1991).
[36]K. Takaki, T. Kise, K. Maruyama, N. Yamanaka, M. Funabashi, and A. Kasukawa, IEEE J. Quantum Electron. **39**, 1060 (2003).
[37]M. Okai, T. Tsuchiya, K. Uomi, N. Chinone, and T. Harada, IEEE Photonics Technol. Lett. **2**, 529 (1990).
[38]Y. Inaba, H. Nakayama, M. Kito, M. Ishino, and K. Itoh, IEEE J. Sel. Top. Quantum Electron. **7**, 152 (2001).
[39]U. Kruger and K. Petermann, IEEE J. Quantum Electron. **24**, 2355 (1988).
[40]X. Pan, B. Tromborg, and H. Olesen, IEEE Photonics Technol. Lett. **3**, 112 (1991).
[41]M. Faugeron, M. Tran, O. Parillaud, M. Chtioui, Y. Robert, E. Vinet, A. Enard, J. Jacquet, and F. Van Dijk, IEEE Photonics Technol. Lett. **25**, 7 (2013).
[42]L. Tombez, S. Schilt, G. D. Domenico, S. Blaser, A. Muller, T. Gresch, B. Hinkov, M. Beck, J. Faist, and D. Hofstetter, in *Conference on Lasers & Electro-Optics Europe & International Quantum Electronics Conference CLEO Europe/IQEC* (IEEE, 2013).
[43]S. Bartalini, S. Borri, I. Galli, G. Giusfredi, D. Mazzotti, T. Edamura, N. Akikusa, M. Yamanishi, and P. De Natale, Opt. Express **19**, 17996 (2011).
[44]A. A. Mills, D. Gatti, J. Jiang, C. Mohr, W. Mefford, L. Gianfrani, M. Fermann, I. Hartl, and M. Marangoni, Opt. Lett. **37**, 4083 (2012).
[45]A. Shehzad, P. Brochard, R. Matthey, T. Südmeyer, and S. Schilt, Opt. Lett. **44**, 3470 (2019).
[46]Y. Deng and C. Wang, IEEE J. Quantum Electron. **56**, 2300109 (2020).
[47]Y. Yu, G. Giuliani, and S. Donati, IEEE Photonics Technol. Lett. **16**, 990 (2004).
[48]J. von Staden, T. Gensty, W. Elsäßer, G. Giuliani, and C. Mann, Opt. Lett. **31**, 2574 (2006).